Mapping Neutron and Proton Drip Lines

Khin Nyan Linn

Abstract

We investigate the position of the neutron and proton drip lines in the framework of the RMF theory with two different parameter sets (NL3 and ChiM). We study the nuclear structure property of all nuclei within the proton and neutron drip lines with the parameter set (ChiM). We compare our theoretical calculation of the drip line nuclei with the experimental data. The boundaries of hypernuclear chart are investigated in spherical calculation as the extensive study for our present work.

I. Introduction

One of the driving forces of today's nuclear physics efforts is the journey to the extreme limits in several directions. For nuclear charge and mass this journey involves nuclei heavier than any that occur in nature or that have been produced in the laboratory, leading the research field of superheavy nuclei; for the neutron-to-proton ratio, it involves the drip lines, the limits of nuclear stability along the axes of proton and neutron number. As more and more neutrons are added to a given nuclide, the neutron binding energy will become eventually negative, leading to the emission of neutrons. The boundary of the region of the (N-Z) plane where this occurs constitutes the "neutron drip line" and its counterpart on the proton rich side, the "proton drip line". The locations of the drip lines on the chart of nuclei are still an open question. In particle accelerators, the existence of about 3,000 isotopes can be studied. [1]. The exact location of the neutron drip line is of great interest in nuclear physics research [9], but the short lifetimes of these exotic nuclei and the difficulty involved in making them results this a tremendous task. Nevertheless, some progress has been made.

The investigation of the proton drip line is easier compared to that of the neutron drip line, because electric repulsion between protons restricts the number that can be added to a nucleus with a given number of neutrons [6]. The procedure is very different for neutron-rich nuclei, because there is no additional electric repulsion by adding neutrons. The neutron drip line is therefore relatively distant from the β stability line on the chart of nuclei, and is therefore much harder to reach experimentally. Furthermore, the number of neutrons that can theoretically be added to a nucleus increases as the number of protons increases.

II. The Relativistic Mean Field Theory

A widespread approximation method for the ground state properties of the finite nuclei is the microscopic self-consistent relativistic mean field theory applying effective interactions. In the present work, we employ the relativistic mean-field (RMF) theory in mean-field approximation and no-sea approximation. Starting from an effective relativistic meson-baryon Lagrangian density and non-relativistic Hartree-Fock (HF) theory with effective interactions, NL3 [8], extended versions including chiral symmetry, ChiM [13], the meson-baryon couplings of RMF theory have been applied. Another well-known feature in the RMF theory is that the proper spin-orbit interaction and associated nuclear shell structure comes out naturally. The proper spin-orbit coupling arises directly from the relativistic nature of the meson-nucleon interactions.

In the walecka-type model, the protons and neutrons are described as Dirac particles interacting in a relativistic covariant manner through the exchange of various mesons including the isoscalar-scalar σ meson, the isoscalar-vector ω meson, the isovector-vector ρ meson and the photon. [11, 14]. In the walecka-type model, the dynamics of a nuclear system which contains the corresponding fields $\psi(x)$ for nucleons, $\sigma(x)$, $\omega^{\mu}(x)$, $\rho^{\mu}(x)$ for mesons and A^{μ} for photons, is determined through the Lagrangian density $\mathcal{L}$ [14],

$$\mathcal{L} = \overline{\Psi}\left(i\gamma_{\mu}\partial^{\mu} - m\right)\Psi + \frac{1}{2}\left(\partial_{\mu}\hat{\sigma}\partial^{\mu}\hat{\sigma} - m_{\sigma}^{2}\hat{\sigma}^{2}\right) - \frac{1}{2}\left(\frac{1}{2}\hat{G}_{\mu\nu}\hat{G}^{\mu\nu} - m_{\omega}^{2}\hat{\omega}_{\mu}\hat{\omega}^{\mu}\right)$$
$$-\frac{1}{2}\left(\frac{1}{2}\hat{\vec{B}}_{\mu\nu}\cdot\hat{\vec{B}}^{\mu\nu} - m_{\rho}^{2}\hat{\vec{\rho}}_{\mu}\cdot\hat{\vec{\rho}}^{\mu}\right) - \frac{1}{4}\hat{F}_{\mu\nu}\hat{F}^{\mu\nu} - g_{\sigma}\hat{\sigma}\hat{\overline{\Psi}}\hat{\Psi} - g_{\omega}\hat{\omega}_{\mu}\hat{\overline{\Psi}}\gamma^{\mu}\hat{\Psi}$$
$$-g_{\rho}\hat{\vec{\rho}}_{\mu}\cdot\hat{\overline{\Psi}}\vec{\tau}\gamma^{\mu}\hat{\Psi} - eA_{\mu}\hat{\overline{\Psi}}\frac{1+\tau_{3}}{2}\gamma^{\mu}\hat{\Psi} - \frac{1}{2}m_{\sigma}^{2}\hat{\sigma}^{2} - \frac{1}{3}b_{2}\hat{\sigma}^{3} - \frac{1}{4}b_{3}\hat{\sigma}^{4}$$

Here, the usual relativistic units of $\hbar$ = c = 1 are used for the discussion of this model [14]. M, m_{σ}, m_{ω}, m_{ρ} are the nucleon-, the σ-, ω-, ρ-meson masses respectively, while g_{σ}, g_{ω}, g_{ρ} and $e^{2}/4\pi$ = 1/137 are the corresponding coupling constants for the mesons and photon. In non-linear versions of the Lagrangian, the coupling is supplemented by a non-linear self coupling of the σ meson, first introduced by Boguta and Bodmer [3] to improve the compressibility of nuclear matter and to obtain a quantitative description of nuclei.

III. Mapping Neutron and Proton Drip Lines

Proton drip line can be defined as the location where the separation energy passes through zero (Sp = 0 MeV) [5]. According to this definition, many nuclei still exist beyond the drip line. An alternative definition of the drip line is described as the value of Z and N for which the last proton is no longer bound and the limitation of the typical nuclear timescale of $\sim 10^{-22}$s which is a reasonable timescale for the existence of a nucleus [10]. The drip line and the existence of a nucleus could also be related to the limitation of radioactivity of $\sim 10^{-12}$ s [8].

The drip lines are the limits of the nuclear landscape where additional protons and neutrons can no longer be kept inside the nucleus and they drip out literally [7]. In our present work, we define the proton drip line as the boundary between the positive value and the negative value of the separation energy. Nuclei inside the drip line are stable with respect to the spontaneous emission of nucleons, whereas these outside the drip lines can spontaneously decay by the emission of one and/or two nucleons.

At a certain line, the nucleus will no longer bind extra neutrons. This is called neutron drip line and its counterpart is called the proton drip line. In other words, an unstable atomic nucleus beyond the drip line will leak free neutrons and the neutron separation energy is zero at the neutron drip line. The proton and neutron drip lines define the limits of existence for finite nuclei. The theoretical knowledge of the properties of nuclei up to the neutron drip line will provide a better understanding of the stellar nucleosynthesis and neutron stars in nuclear astrophysics.

The position of the drip lines is still uncertain and its experimental determination is a problem of foremost interest in the field. Baumann and et. al., reported a significant advance in the determination of the neutron drip line: the discovery of two neutron-rich isotopes ^{40}Mg and ^{42}Al that are predicted to be drip line nuclei [2]. The discovery of ^{40}Mg as the neutron drip line nucleus and the most recently observed drip line nucleus ^{44}Si are in agreement with our prediction of neutron drip line by applying the RMF theory with the parameter set ChiM.

From Fig. 1, we can observe that the proton drip line is closer to β stability line than the neutron drip line in both parameter sets. The neutron drip line (calculated with the parameter set NL3) is relatively distant from that of another parameter set ChiM. With the parameter set NL3, the prominent shell closure can be observed in this result.

As an extensive study of investigation of normal drip lines, we also carried out the stability limits of hypernuclei in spherical calculation with two different parameter sets. From these calculation, one can observe that both proton and neutron drip lines with the inclusion of Λ

hypernuclei move towards the neutron rich sides from the drip lines of nuclei without Λ. From these results, we can conclude that hypernuclei can accept more neutrons and are more strongly bound than normal nuclei. These results are useful to understand the structure of the nucleus and more specifically, physics close to the drip lines.

IV. Study of Nuclei within Proton and Neutron Drip Lines

The RMF theory with ChiM parameter set can reproduce the deformations of finite nuclei very well. In the present work, we performed the quadrupole deformation for all even-even nuclei with $8 \leq Z \leq 100$ between the proton and neutron drip lines. From the analysis of this calculation, we can conclude as follows:

Most of the spherical nuclei ($-0.05 \leq \beta_2 \leq 0.05$) are located at or near magic numbers. While isotonic change with well-known neutron magic numbers (N =82, 126, 184) preserve spherical shapes for the entire chain, isotopic chain with proton magic numbers are usually deformed when one moves away from the neutron magic numbers (except for the Z = 8 and 20 isotopic chain). Among these results, we can observe well-known doubly magic nuclei (^{16}O, ^{40}Ca, ^{48}Ca, ^{132}Sn, ^{208}Pb) except for the (Z = 28 isotopic chain). Most of prolate deformed nuclei are observed in the nuclei with a charge larger than Z = 50 when moving away from the magic numbers either isotonically or isotopically. Oblately deformed nuclei are rare. There are some oblate regions in this axially deformation of even-even nuclear chart.

One of oblate deformed regions is described in Fig. 2. This oblately deformed region lies among the isotonic changes of Zn isotopes (Z = 30) to Kr isotopes (Z = 36). From this region, we can observe that the oblate ground state and prolate excited state nuclei. These nuclei are quite deformed nuclei ($-0.2 \leq \beta 2 \leq -0.3$).

V. Summary

We have investigated the position of neutron and proton drip lines in the relativistic mean field model with two parameter sets. Reasonable agreement with the available experimental data is described. The general feature of the nuclear deformations was studied within proton and neutron drip lines. The limits of hypernuclear stability in spherical calculation are performed. A more detailed study of the results of the present calculation is in progress.

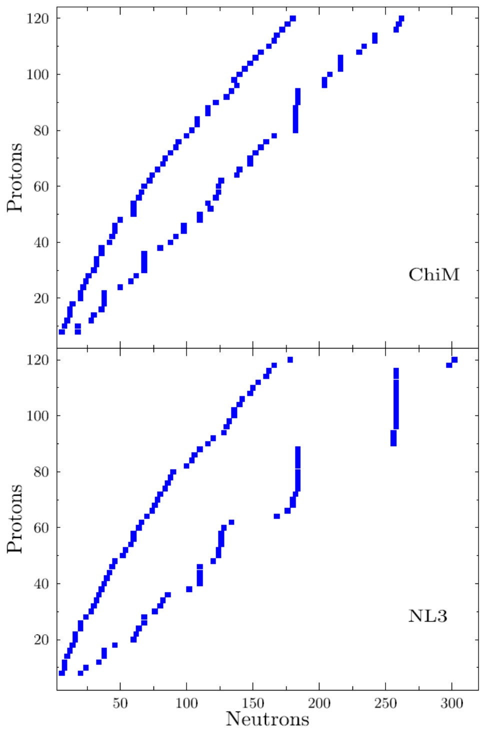

Fig. 1. Neutron and proton drip lines calculated by RMF theory with two parameter sets ChiM and NL3.

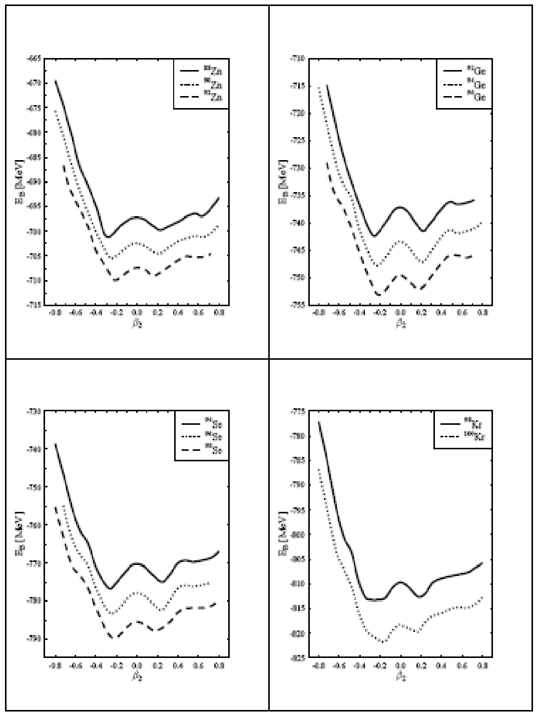

Fig. 2. Deformation β_2 in oblate deformation (Z = 30 to 36) region

VI. Acknowledgement

We all thank to professor Dr. Aye Aye Lwin for pointing to the interest in our work and her continuous encouragement. The author, Khin Nyan Linn thanks to professor Dr. Stefan Schramm and Dr. Thomas J Bürvenich for their supervision and discussion. This work was supported by DAAD (Deutscher Akademischer Autauschdienst).

[1] Audi, G., Wapstra, A. H. and Thibault, C. Nucl. Phys. A. 729, 337 (2003).

[2] Baumann, T. and et al., Nature 449, 1022 (2007).

[3] Boguta, J. and Bodmer, A. Nucl. Phys. A. 292, 413 (1977).

[4] Cerny, J. and Hardy, J. Ann. Rev. Nucl. Part. Sci. 27, 333 (1977).

[5] Hansen, P. G. and Tostevin, P. G. Ann. Rev. Nucl. Part. Sci. 53, 219 (2003).

[6] Heenen, P.-H. Nature 449, 992 (2007).

[7] Jonson, B. Phys. Rep. 389, 1 (2004).

[8] Lalazissis, G. A., König, J. and Ring, P. Phys. Rev. C. 55, 540 (1997).

[9] Lunney, D. , Pearson, J. M. and Thibault, C. Rev. Mod. Phys. 75, 1021 (2003).

[10] Mueller, A. C. and Sherrill, A. C. Ann. Rev. Nucl. Part. Sci. 1993, 529 (43).

[11] Reinhard, P. G. Rept. Prog. Phys. 52, 439 (1989).

[12] Reinhard, P. G. and Flocard, H. Nucl. Phys. A. 584, 467 (1995).

[13] Schramm, S. Phys. Rev. C66, 064310 (2002).

[14] Serot, B. D. and Walecka, J. D. Adv. Nucl. Phys. 16 (1986).

[15] Sharma, M. M. and et al., Phys. Rev. Lett. 72, 1431 (1994).